STAR★METHODS

KEY RESOURCES TABLE

REAGENT or RESOURCE	SOURCE	IDENTIFIER
Biological samples		
Ancient skeletal element	This study	PAPV26
Ancient skeletal element	This study	PAPV27
Ancient skeletal element	This study	PAPV52
Ancient skeletal element	This study	PAPV53
Ancient skeletal element	This study	PAPV57
Ancient skeletal element	This study	PAPV61
Ancient skeletal element	This study	PAPV93
Ancient skeletal element	This study	PAPV106
Ancient skeletal element	This study	PAPV109
Ancient skeletal element	This study	PAPV114
Ancient skeletal element	This study	PAPV117
Ancient skeletal element	This study	PAPV118
Ancient skeletal element	This study	PAPV137
Ancient skeletal element	This study	PAPV146_FE
Ancient skeletal element	This study	PAPV146_TP
Ancient skeletal element	This study	PAPV156
Ancient skeletal element	This study	PAPV167
Ancient skeletal element	This study	PAPV172
Ancient skeletal element	This study	PAPV173
Ancient skeletal element	This study	PAPV174
Ancient skeletal element	This study	PAPV175
Chemicals, peptides, and recombinant proteins		
NEBNext Multiplex Oligos for Illumina (Index Primers Set 1)	New England Biolabs	E7335L
NEBNext Multiplex Oligos for Illumina (Index Primers Set 2)	New England Biolabs	E7500L
NEBNext Multiplex Oligos for Illumina (Index Primers Set 3)	New England Biolabs	E7710L
NEBNext Multiplex Oligos for Illumina (Index Primers Set 4)	New England Biolabs	E7730L
NEBNext Multiplex Oligos for Illumina (Dual Index Primers Set 1)	New England Biolabs	E7600
NEBNext Multiplex Oligos for Illumina (Methylated Adaptor, Index Primers Set 1)	New England Biolabs	E7535L
NEBNext Multiplex Oligos for Illumina (96 Index Primers)	New England Biolabs	E6609L
NEBNext High-Fidelity 2X PCR Master Mix	New England Biolabs	M0541L

(*Continued on next page*)

Continued

REAGENT or RESOURCE	SOURCE	IDENTIFIER
Phusion High-Fidelity PCR Master Mix with HF Buffer	New England Biolabs	M0531L
Blunt-TA Ligase Master Mix	New England Biolabs	M0367
Buffer PE (concentrate, 100 ml)	QIAGEN	19065
Buffer EB (250 ml)	QIAGEN	19086
TE buffer, pH 7.6, RNase free (250 ml)	Carlo Erba	LJ62285AK
Tween* 20	Carlo Erba	ABP337-500
Sodium Acetate	Carlo Erba	478166
Nuclease-free water	Promega	P1193
Bleach 100%	Aurogene	AU1125
Isopropanol	Carlo Erba	415154
EDTA 0.5 M	Carlo Erba	LJ62786AK
Proteinase K	Merck	3115852001
10% N-lauryl sarcosine	Merck	8147150100
Guanidine hydrochloride	Carlo Erba	A120232500
GoTaq(R) Long PCR Master Mix	Promega	M4021
Critical commercial assays		
Axiom Genome-Wide Human Origins 1 Array	Thermo Fisher Scientific	901853
NEBNext Ultra DNA Library Prep Kit for Illumina	NEB-Euroclone	BE7645S
MinElute Reaction Cleanup Kit	QIAGEN	28206
Qubit dsDNA HS Assay Kit	Thermo Fisher Scientific	Q32851
MiSeq Reagent Kit v2	Illumina	MS-102-2002
Nextera XT DNA Library Preparation Kit	Illumina	FC-131-1096
Maxwell RSC Stabilized Saliva DNA Kit	Promega	AS1630
Software and algorithms		
OxCal	Ramsey and Lee, 2013	https://c14.arch.ox.ac.uk/oxcal.html
CutAdapt	Martin, 2011	https://github.com/marcelm/cutadapt
FastQC	Andrews, 2010	https://www.bioinformatics.babraham.ac.uk/projects/fastqc/
BWA	Li and Durbin, 2010	http://bio-bwa.sourceforge.net/
Picard MarkDuplicates	http://broadinstitute.github.io/picard	http://broadinstitute.github.io/picard
MapDamage2.0	Jónsson et al., 2013	https://ginolhac.github.io/mapDamage/
ANGSD	Korneliussen et al., 2014	https://github.com/ANGSD/angsd
READ	Monroy Kuhn et al., 2018	https://bitbucket.org/tguenther/read/src/master/
KING	Manichaikul et al., 2010	http://people.virginia.edu/~wc9c/KING/
PLINK1.9	Purcell et al., 2007	https://www.cog-genomics.org/plink/2.0/
ADMIXTURE	Alexander et al., 2009	http://dalexander.github.io/admixture/index.html
RFMix	Maples et al., 2013	https://sites.google.com/site/rfmixlocalancestryinference/
CircularMapper	Peltzer et al., 2016	https://github.com/apeltzer/CircularMapper
SAMtools	Li et al., 2009	http://samtools.sourceforge.net/
BCFtools	Li et al., 2009	http://samtools.github.io/bcftools/bcftools.html
VCFtools	Danecek et al., 2011	http://vcftools.sourceforge.net/
HaploGrep2	Weissensteiner et al., 2016	https://github.com/seppinho/haplogrep-cmd
GATK	McKenna et al., 2010	https://gatk.broadinstitute.org/hc/en-us
BEAST	Bouckaert et al., 2019	http://beast.community/
Tracer	Rambaut et al., 2018	http://tree.bio.ed.ac.uk/software/tracer/

(*Continued on next page*)

Continued

REAGENT or RESOURCE	SOURCE	IDENTIFIER
FigTree	http://tree.bio.ed.ac.uk/software/figtree/	http://tree.bio.ed.ac.uk/software/figtree/
Yhaplo	Poznik, 2016	https://github.com/23andMe/yhaplo
EIGENSOFT	Patterson et al., 2006	https://github.com/DReichLab/EIG
CLUMPAK	Kopelman et al., 2015	http://clumpak.tau.ac.il/
DISTRUCT	Rosenberg, 2004	https://rosenberglab.stanford.edu/distruct.html
AdmixTools	Patterson et al., 2012	https://github.com/DReichLab/AdmixTools
TreeMix	Pickrell and Pritchard, 2012	https://bitbucket.org/nygcresearch/treemix/wiki/Home
qpGraph	Patterson et al., 2012	https://github.com/DReichLab/AdmixTools
SHAPEITv2	Delaneau et al., 2011	https://mathgen.stats.ox.ac.uk/genetics_software/shapeit/shapeit.html
CHROMOPAINTERv2	Lawson et al., 2012	http://www.paintmychromosomes.com/
fineSTRUCTURE	Lawson et al., 2012	http://www.paintmychromosomes.com/
Refined-IBD	Browning and Browning, 2013	http://faculty.washington.edu/browning/refined-ibd.html
IBDne	Browning et al., 2018	http://faculty.washington.edu/browning/ibdne.html
ContaminationX	Moreno-Mayar et al., 2020	https://github.com/sapfo/contaminationX
ContamMix	Fu et al., 2013	-
Schmutzi	Renaud et al., 2015	https://github.com/grenaud/schmutzi
Rx	Mittnik et al., 2016	Mittnik et al., 2016
Qpwave	Reich et al., 2012	https://github.com/DReichLab/AdmixTools
Deposited data		
Mitogenomes of Modern Individuals	GenBank	MW467798-MW467881
Genotype Data of Modern Individuals	Mendeley Data	https://doi.org/10.17632/d45xg84bcj.1
Sequencing Data of Ancient Individuals	European Nucleotide Archive	PRJEB42372

See specific file.

RESOURCE AVAILABILITY

Lead contact

Further information and requests for resources and reagents should be directed to and will be fulfilled by the Lead Contact, Alessandro Achilli (alessandro.achilli@unipv.it).

Materials availability

This study did not generate new unique reagents.

Data and code availability

The accession number for the ancient DNA sequencing data reported in this paper is ENA: PRJEB42372. Modern genotype data have been deposited to Mendeley Data: https://doi.org/10.17632/d45xg84bcj.1. The accession numbers for modern complete mitogenomes reported in this paper are GeneBank: MW467798-MW467881. Scripts used to infer Y chromosome aDNA haplogroups are available on GitHub (https://github.com/raveancic/aDNAYchromosome), all the other scripts used for analysis and plots are available upon request.

EXPERIMENTAL MODEL AND SUBJECT DETAILS

Insights into pre-Hispanic Panama: details on archaeology, history, and linguistics

From ca. 4.5 kya agriculture along Panama's Pacific watershed was complemented by fishing in rivers and estuaries, and catching birds, large snakes and iguanas (*Iguanidae spp.*), and hunting mammals with body masses < 55 kg on the offshore Pearl Island archipelago (Cooke et al., 2016). Some of these, e.g., white-tailed deer (*Odocoileus virginianus*), raccoons (*Procyon lotor*) and rodents

including agouti (*Dasyprocta punctata*) and paca (*Cuniculus paca*), forage in human trash and eat crops in gardens and fields (Cooke et al., 2007, 2008; Martínez-Polanco et al., 2020). On *Pedro Gonzalez* (Pearl Islands), a very small deer (*Mazama sp*.) (7-10 kg) was extirpated by hunting. Dolphins (*Tursiops and Delphinus*) were consumed 6.2-5.6 kya and were possibly killed when beached (Cooke et al., 2016). Later, with the establishment of villages ca 4-2 kya, community activities diversified, especially regarding the exchange of goods. Hunting strategies now included communal drives in Pacific wooded savannas. Deer meat was stored salted and dried and then served at special feasts (Martínez-Polanco and Cooke, 2019).

Inhabitation of the Caribbean side of the Central American Isthmus (Costa Rica) began in the Late Pleistocene (13.4-12 kya) (Ranere and Cooke, 2020). In the very humid central Caribbean Panama, human activities date back to 5.9 kya when groups crossed the Central Cordillera to collect food and materials not available on the opposite side, e.g., embalming agents.

On the central Caribbean, maize is found in rock shelters with earth ovens from about 3.5 kya. Materials analysis demonstrates that Monagrillo pottery found here was manufactured in the central Pacific watershed (Griggs, 2005; Iizuka et al., 2014). One site in the coastal lowlands of Coclé province (Zapotal, PR-32), which used Monagrillo pottery, consisted of dwellings stratified within a shell-bearing midden accumulated between 4.3 and 3.2 kya. Zapotal has the characteristics of a small village. There are very large numbers of edge-ground cobbles here, which were used at many 8-3 kya sites in Panama for grinding several plant foods including maize and manioc. The abundance of small fish (< 300 g live weight) that were taken at Zapotal points to the use of tidal traps and weirs in the nearby estuary in order to maximize biomasses (Zohar and Cooke, 2019).

By 3 kya notable differences had arisen in the material culture of a western region (Greater Chiriquí; Chiriquí and Bocas del Toro provinces) and a central region (Greater Coclé; Coclé, Azuero Peninsula and Veraguas provinces). Greater Chiriquí shows material culture, art, genes and language that are broadly consistent (Ulloa, 2017), in distinction to the Greater Coclé or the even more diverse, but less studied, Greater Darién.

Unique ceremonial and religious precincts stand out in both the Chiriquí and Coclé cultural areas, although they are markedly different: Barriles in highland Chiriquí (Linares et al., 1975), and the twin sites of Sitio Conte and El Caño in the Pacific Coclé lowlands. The ceremonial site at Barriles consists of low platforms, boulder petroglyphs, urn burials, large statues depicting one man sitting on another's shoulders–in an apparent display of social dominance–and an enormous maize-grinding stone (metate) showing explicit iconographic connections between maize and human fertility (Linares et al., 1975). Maize, beans (*Phaseolus* spp,), and palm and tree fruits characterize the samples of carbonized plant remains in the middens in domestic areas (Dickau, 2010; Smith, 1980).

The Barriles ceremonial precinct seems to have served many communities located between 1,000 and 2,300 m above sea level in the shadow of the Barú volcano, which last erupted 0.5 kya (Holmberg, 2007). It is inferred that Barriles was the initial settlement of a cultural group that first entered this highland zone from elsewhere ca 2.8 kya. Friction led to fission. A sector of the colonizing population moved to Cerro Punta and henceforth maintained vacillating relations with its ancestors (''peace, trade, war''). Communion among the entire descent group was not severed. Periodically, perhaps annually, festivals were held at ancestral Barriles. The feats of the founders and supernatural helpers were celebrated. Large quantities of alcoholic beverages (e.g., maize and palm sap) were likely brewed.

The well-studied heritage of Greater Coclé, which reached its apogee at the great ceremonial and burial precincts of Sitio Conte and El Caño 1.5–0.95 kya (Lothrop, 1937, 1942; Mayo Torné, 2015), confirms a continuity of iconography and symbolism on decorated pottery from 2.5 kya until two decades after Spanish conquest in this central region. But whether this area was also linguistically united cannot yet be determined.

Cultural geography becomes even more complex in the Greater Darién area extending from the El Valle Pleistocene volcano to eastern Darién. Historians and most archaeologists agree that by 1,500 CE the eastern region, and possibly much of the central area, was inhabited by speakers of the Cueva language. Historian Kathleen Romoli and linguists Jacob Loewen and Adolfo Costenla have proposed for many years that the group of settlements that at the time of Spanish conquest spoke the ''language of Cueva'' were not an ''ethnic group'' but, rather, a collection of settlements that shared the Cueva language as a *lingua franca*. These three researchers also argue that some polities in fact spoke variants of languages in the Chocoan family, especially those on the Pacific side of the Isthmus (Costenla, 2012; Loewen, 1963; Romoli, 1987). Chibchan languages probably derive from a proto-language that coalesced about 10 kya (O'Connor and Muysken, 2014) in a ''core area'' on the lower Central American Isthmus (southern Costa Rica and western central Panama). Ever since Barrantes et al. (1990) conducted an isozyme-based study of modern Central American Indigenous polities that spoke languages in the Nuclear Chibchan family (Costenla, 2012), it has been apparent that this population coalesced very early in the Holocene and at the onset of agriculture gradually experienced *in situ* fission and fusion.

Ceramics found in eastern Panama point to greater proximity to the Greater Coclé tradition than a putative Gran Darién cultural sphere among the peoples who inhabited this region from 200 BCE to 1200 CE. Recent findings on the Pearl Islands archipelago confirm the expansion of the ceramic style known as Cubitá, as well as molded and incised variations of the Conte style, both from the central region of Gran Coclé in the gulf of Panamá (Martín et al., 2016). Biese had already suggested that this expansion reached *Panamá Viejo*, where he reported examples of the Conte style excavated around Puente del Rey, toward the north of the site (Biese, 1964).

At the Miraflores site on the Banks of the Bayano River (Cooke, 1976; Oyuela-Calcedo and Raymond, 1998), 670–1015 CE and 700–1030 CE according to the latest 2 sigma calibrations (Martín et al., 2016), only one piece made in the region exhibited painted decorations with obvious influences from Greater Coclé: a plate with a tripod pedestal with the effigy of a monkey (Cooke, 1998). The same pattern of cultural replacement is documented on the Pearl Islands archipelago, where the islands' Fifth Ceramic Horizon is

identified from 750 through 1350 CE (Martín et al., 2016). This late ceramic configuration, which features incised decoration and molding procedures different from its immediate precedents, is that which archaeologists normally associate with Greater Darien, the region that sixteenth-century Spanish chroniclers described as populated by communities that spoke the ''Cueva language'' from Urabá to the eastern slope of the El Valle volcano (Martín, 2002b; Romoli, 1987).

Martín et al. (2016) argue that the discrepancy between the Greater Darien and Greater Coclé cultural areas, whose geographical extension may have shifted over time, could derive from a change in the population inhabiting the Pearl Islands archipelago: the group using Cubitá ceramics and Conte variations may have ceded before the entry of a population with a very different ceramic tradition from the Darien region and related to northwest Colombia. Another hypothesis (Cooke, 1998; Martín and Sánchez, 2007; Sánchez-Herrera and Cooke, 2000) relates the changes observed to a reorganization of the commercial routes and exchanges from 500 CE, which intensified after 800-900 CE, with the introduction of metallurgy to the isthmus and the replacement of shell artifacts with those of gold to represent high social status. From at least the beginning of the common era through the end of its first millennia, the dispersion of Cubitá ceramics allude to the fact that the Pearl Islands archipelago, the Azuero Peninsula and the central coast of the bay of Panama participated in the same sphere of social interaction. This relationship changed completely in the subsequent period, and until European contact.

The uneven impact of European colonization and the upheaval it induced, in addition to subsequent migrations, show that comprehensive and detailed studies of this time period need to be completed in this region to help trace population histories of Indigenous groups before and after 1500 CE. Although goods also crossed the isthmus in pre-colonial times, the process intensified after the early sixteenth century, when the Spanish established settlements on both sides of the Isthmus to forge a highway for the global transit (and often forced mobility) of persons and goods between the Atlantic and Pacific Oceans.

Ancient Individuals and archaeological information

In order to assess change and continuity in the most radically transformed area of the Isthmus, the under-studied eastern region, 20 ancient individuals (21 specimens in total, sometimes referred as ancient Panamanians for the sake of clarity) were collected from seven different archaeological excavations (six of these within today's *Patronato Panamá Viejo*, and one at nearby *Coco del Mar*) (Figure 1A; Table S1). Based on the style of the ceramics recovered, archaeologists consider the area related to contiguous contemporary settlements as part of an extended pre-Hispanic presence of Cueva-speakers within the Greater Darien cultural region (Martín, 2002b). This population coexisted and mixed with Spanish settlers from 1519 to 1541 Common Era (CE), as an Indigenous presence among Old Panama's earliest Christian burials suggests. The excavations sampled took place in and near Panamá Viejo, the site of the colonial city from 1519 through 1671 CE, and an area of pre-Hispanic occupation before that.

1. Plaza Mayor (N = 4)

The burial site excavated in the Plaza Mayor, originally identified as *Tumba 1* (Figure 1B), contained the remains of a female individual with a spondylus necklace and surrounded by offerings that included nine male crania. Scholars have awaited genetic research in order to test the hypothesized relationships regarding the individuals buried within this tomb since its discovery in 1996 (Mendizabal, 2004). DNA was successfully extracted from the main individual (PAPV109) and three of the nine skulls (PAPV114, 117 and 118) around her. PAPV109 did not meet quality standards to be included in autosomal analyses (Table S1).

2. Plaza Casas Oeste (N = 1)

In the Plaza Mayor's Casas Oeste, the remains of 35 pre-Hispanic individuals were found in different positions, including extended burials, as well as urns and packages of bones. DNA of one of these individuals (PAPV137), radiocarbon dated 898-1014 (2 sigma), a male individual of at least 15 years at death, extended yet leaning toward the right side, with his skull pointed northwest, was extracted in this work.

3. Catedral (N = 5)

Human remains excavated from Old Panama's Cathedral in Panamá Viejo (PAPV52, 53, 57) and its courtyard (PAPV61, 93) in 2000 reflect the African and European presence, as well as a mixed Indigenous inheritance, in the city from 1542 to 1671 CE (Hernández Mora et al., 2021).

4. Sur de la Plaza (N = 2)

Two post-contact individuals analyzed here were excavated from Sur de la Plaza (PAPV26, 27) and dated 1519-1541 CE, based on the historical and archaeological evidence.

5. Parque Morelos (N = 4)

Other pre-Hispanic burials were excavated from the Parque Morelos (roughly 1 km to the west of the Plaza Mayor) in 2001-2003. These excavations uncovered the remains of two pre-Columbian residential structures, including evidence of post-holes, pottery, grinding stones, seashell beads, fragments of three bone flutes and a frog-shaped gold pendant. Within a few meters from the residential structures, urns and ''packages'' with cranial and long bones belonging to children and adults (PAPV146 and 156, dated 776-966 and 1264-1289 CE, respectively, and the first one with DNA extracted from two different bones), were also recovered (Martín, 2002a, 2006). An additional individual was excavated in an extended primary burial (PAPV167, 779-985 CE, 2 sigma) some 50 m from the residential structures.

6. Centro de Visitantes (N = 1)

Another pre-Hispanic individual was extracted from an extended burial excavated by Juan Martín in 2001 at the Centro de Visitantes site, close to Parque Morelos, in the west part of Panamá Viejo (PAPV106), and dated 894-986 CE (2 sigma). Five ceramic offerings accompanied this female individual, of approximately 30-35 years at death.

7. Coco del Mar (N = 4) located outside Panamá Viejo

The additional site where pre-Hispanic human remains were uncovered in 2005 was in an adjacent residential area, *Coco del Mar*, one kilometer to the west of the *Morelos* statue. In this case, the burial is characterized by a particular conformation (Figure 1B), where a primary, female individual (PAPV172) was discovered with three male crania (PAPV173, 174, 175) and additional pottery as offerings (Martín et al., 2008), similar to that of Plaza Mayor's *Tumba 1*.

Modern Individuals

In 2010, Indigenous polities encompassed about 12% of the 3.4 million inhabitants of Panama. The most numerous are individuals who identify as the Ngäbe (62.3%), Guna (19.3%) and Emberá (7.5%), followed by smaller polities such as the Chocoan-speaking Wounaan (the Noanomá of Spanish chronicles), and the Buglé, Bribri, and Naso Djërdi (formerly known as Teribe). The contemporary population also includes important numbers of self-identified Afro-Panamanians ("Morenos") and individuals of mixed Hispano-Indigenous ("Mestizo") ancestry.

Modern sampling took place in Panama City as well as in the provinces and Indigenous territories. A total of 84 biological samples were collected in Panama from healthy adult (> 18 years old) individuals, almost equally distributed between females and males (41 and 43, respectively), and belonging to different Indigenous groups using NorgenBiotek kits (Figure 1A; Table S1). During sample collection, genealogical information (for at least two generations), cultural affiliation, and spoken language were also gathered from each subject.

METHOD DETAILS

Collagen extraction and ^{14}C-dating

The individuals PAPV106, PAPV109, PAPV114, PAPV117, PAPV118, PAPV137, PAPV146, PAPV156, PAPV167, PAPV172, PAPV173, PAPV174 and PAPV175 were analyzed by accelerator mass spectrometry (AMS) at Mannheim (Table S1) together with additional individuals from the same sites, i.e., PAPV110, PAPV111, PAPV112, PAPV113, PAPV115, PAPV116, PAPV139, and PAPV 169, dated between 990 and 1,385 CE (https://artempire.cica.es/archeo/list), with an overall time span from 603 to 1,430 CE.

Compact bone portions were cut and the surfaces removed. About 1 g of sample was placed in glass tubes, demineralized in 10 mL of 0.5 N HCl at initially 4°C and later at room temperature for 14 days, rinsed to neutrality and reacted with 10 mL of 0.1 M NaOH for 24 h at 4°C, rinsed again to neutrality and gelatinized in 4 mL of acidified H_2O (pH 2-3) for 48 h at 75°C. Insoluble particles were separated using EZEE filter separators. Ultrafiltration (molecular mass > 30 kD) removed the short-chained collagen and concentrated the long-chained collagen, which was frozen and lyophilized.

The collagen was combusted and the relative amounts of carbon (C) and nitrogen (N) determined using an elemental analyzer (Elementar Inc., MicroCube). The produced CO_2 was reduced to graphite using either a custom-made, semi-automated graphitization unit or a fully automated and commercially available unit (IonPLus Inc., AGE3). The resulting graphite powder was compressed into aluminum targets and subsequently analyzed using a MICADAS-type AMS-system (IonPlus Inc.) (Kromer et al., 2013).

The isotopic ratios $^{14}C/^{12}C$ and $^{13}C/^{12}C$ of samples, calibration standard (Oxalic Acid-II), blanks and control standards were measured simultaneously in the AMS. ^{14}C-ages were corrected for isotopic fractionation to $\delta^{13}C = -25‰$ (Stuiver and Polach, 1977) using the $^{13}C/^{12}C$ AMS-values and calibrated using the dataset INTCAL13 (Reimer et al., 2013, 2020) and software SwissCal (L.Wacker, ETH-Zürich). Calibration graphs were generated using the software OxCal (Ramsey and Lee, 2013).

Ancient DNA processing

Different bones (femur, humerus and petrous bone) and teeth were available from ancient individuals for DNA extraction (Table S1), which was carried out in the dedicated clean rooms at the Carl R. Woese Institute for Genomic Biology, University of Illinois, following published protocols (Dabney et al., 2013; Lindo et al., 2017; Pinhasi et al., 2015; Scheib et al., 2018). Bones or teeth were soaked in sodium hypochlorite (bleach 100%) for 3 minutes to remove surface contamination, then washed three times with DNA-free ddH_2O and once with isopropanol. Dried samples were placed in a DNA Crosslinker under UV. About 0.1 g of tooth or bone powder were drilled. The powder was incubated in 1 mL of 0.5 M EDTA with 60-100 μl of Proteinase K (33.3 mg/ml) and 50 μl of 10% N-lauryl sarcosine for 20-24 hours at 56°C. The digested samples were concentrated at ~100 μl using Amicon centrifugal filter units. The DNA was purified using the MinElute Reaction Cleanup Kit (QIAGEN). The extracted DNA was quantified with Qubit dsDNA HS Assay Kit and tested through a PCR amplification of mtDNA control-region fragments (< 150 bps). Samples showing at least 5 ng of DNA and with at least one successful short mtDNA amplification were selected for shotgun sequencing.

Double-stranded DNA libraries were prepared starting from ~55.5 μl of extracted DNA using the NEBNext® Ultra DNA Library Prep Kit for Illumina®. Adapters were used in a dilution of 1:20, which is recommended for low concentration DNA samples. Adaptor-ligated libraries were purified using the MinElute Reaction Cleanup Kit (QIAGEN) and then prepared for amplification, which was car-

ried out in thermocyclers in the modern DNA laboratory. The MinElute Reaction Cleanup Kit (QIAGEN) was used to clean amplified libraries, whose quality was then checked on the E-Gel Precast Agarose Electrophoresis System and quantified on the Agilent 2100 Bioanalyzer Instrument with the High Sensitivity DNA kit.

Eventually, 21 DNA libraries (10 nM) were selected (two for the individual PAPV146) for Illumina sequencing on the HiSeq4000 (single-end 100 bp, for a total of 150-200M reads) at the Roy J. Carver Biotechnology Center of the University of Illinois.

Mitochondrial DNA capture was also performed at the University of Florence for four individuals (PAPV27, PAPV53, PAPV93, PAPV109), as in (Modi et al., 2020).

Modern DNA processing

After automated DNA extraction with Maxwell® RSC Instrument in the lab of Genomics of Human and Animal Populations at the University of Pavia, the samples were genotyped with the Affymetrix Human Origin 600K chip at the Institute of Healthcare Research in Santiago de Compostela (CEGEN).

As for the mitogenome sequencing, the entire mtDNA was amplified in two overlapping fragments (Modi et al., 2020). Libraries were prepared using the Illumina Nextera XT DNA preparation kit and sequenced at the National Neurological Institute C. Mondino in Pavia on an Illumina MiSeq instrument (paired-end reads 150x2).

QUANTIFICATION AND STATISTICAL ANALYSIS

Ancient data preparation for analysis

Illumina adapters were removed from raw data using CutAdapt (Martin, 2011). Trimmed FASTQ files were then checked with FastQC (Andrews, 2010). Taking into account the high number of K-mers that were found, mostly poli-A probably generated during the blunt-end phase, CutAdapt was run twice to remove these artifacts. Trimmed reads were mapped against the human reference genome hg19 build 37.1, as well as versus the revised Cambridge Reference Sequence (rCRS) in separate runs, using the algorithm *aln* of bwa v0.6.1 (Li and Durbin, 2010). The numerous duplicates, generated during library amplification, were removed with the tool MarkDuplicates of the Picard package (http://broadinstitute.github.io/picard).

Validation tests

Ancient DNA damage pattern. Damage patterns (Table S2) were analyzed with MapDamage2.0 (Jónsson et al., 2013). The molecular decay after death was calculated from the length of the reads, as in (Allentoft et al., 2012). We used the error rate estimate to confirm the antiquity of our reads (Table S2). It calculates the excess of derived alleles observed in an ancient genome (compared to a high-quality genome) taking into account that all the anatomically modern humans should have the same percentage of derived alleles. The error rate analysis was performed comparing our trimmed FASTQ with the "Error estimation" tool of ANGSD (Analysis of Next Generation Sequencing Data) (Korneliussen et al., 2014), using the chimp genome as an outgroup and the genome NA12778 (from the 1000 genomes project), as an error-free individual (Schroeder et al., 2018).

To double-check if an excess of damage and/or erroneous adapters' trimming might affect the results of the subsequent analyses, we repeated two AncientPanama FASTQ trimming using more stringent criteria: removing 10 additional bases from both ends of each read; removing the adapters using a higher mismatch rate (up to 50%) than in the original pipeline (20%). These trimmed FASTQ were then mapped against the reference genome hg19 build 37.1. We repeated the specific Isthmo-Colombian PCA analysis including the Ancient Panamanian data trimmed with more stringent criteria finding consistent results with the original plot in Figure 2B.

Contamination tests

Chromosome X contamination. For each library derived from ancient male individuals we estimated nuclear contamination using the approach described in Moreno-Mayar et al. (2020), based on reads mapping to the X chromosome. This method relies on the fact that males are hemizygous for X-linked loci outside the pseudo-autosomal regions, making multiple alleles in these loci attributable to either errors or contaminations. These estimates can be used as proxy for nuclear contamination estimates in ancient male individuals.

We used ANGSD (Korneliussen et al., 2014) to estimate contamination on reads with mapping quality greater than 30 and base quality greater than 20. We considered at least 100 sites with depth greater than or equal to 2 (Nägele et al., 2020) matching the HapMap CEU allele frequencies (Altshuler et al., 2010) as potential contaminants, after excluding pseudo-autosomal regions on chromosome X. We then applied the tool presented in Moreno-Mayar et al. (2020) to estimate contamination using low-depth X chromosome data, setting to 1,000 the maximum number of jackknife samples used for estimating standard errors and considering the estimates from the Two-consensus method.

Mitochondrial DNA contamination. Jones's method: Contamination in ancient mitochondrial sequences was first estimated by assessing the number of non-consensus base calls (with base quality greater than or equal to 20) at haplogroup diagnostic positions as a function of the total coverage for each of these sites (Jones et al., 2017).

contamMix: We also estimated mtDNA contamination in our data by using contamMix v. 1.0-10, which provides the maximum *a posteriori* probability of the consensus sequence being authentic (Fu et al., 2013). This method is based on the reconstructed mtDNA consensus to estimate contamination, which should not exceed 50% for contamMix to work. First, we built an mtDNA consensus sequence running ANGSD (Korneliussen et al., 2014) and using the parameters -doCounts 1 and -doFasta 2 (majority rule). We retained only reads with mapping quality higher than 30 and nucleotides with base quality greater than 20. Moreover, we filtered for

sites with a minimum depth of 5X. Then, we remapped to the rebuilt consensus sequence only the reads that mapped uniquely to the mitochondrial reference sequence. We used mafft (Katoh et al., 2002; Katoh and Standley, 2013) to align our consensus sequence to a panel of 311 worldwide mtDNA sequences (Green et al., 2008), representing potential contaminant sequences. Finally, we used both the alignment and the remapped reads for contamination estimation with contamMix, running five independent chains for 50,000 iterations. The results were checked by monitoring the Gelman diagnostic (Gelman and Rubin, 1992) to confirm convergence.

Schmutzi: The third method to estimate mtDNA contamination was Schmutzi (Renaud et al., 2015), which jointly estimates present-day human contamination and reconstructs the endogenous mitochondrial sequence by considering both deamination patterns and fragment length distributions. Present-day human contamination was evaluated by an iterative likelihood method implemented in Schmutzi using a non-redundant database of 197 human mitogenomes available in the software package.

Molecular sex and kinship determination

The sex of each individual was determined using two computational approaches specific for low-coverage genomes, Ry (Skoglund et al., 2013) and Rx (Mittnik et al., 2016) (Table S2). The relationships between the ancient Isthmian individuals were verified using the tool READ with default parameters (Monroy Kuhn et al., 2018) (Table S2).

Checking for reference bias

The reference bias indicates an increased probability of detecting the alleles present in the reference sequence, especially when dealing with paleogenomic data affected by fragmentation and other post-mortem damage, often generating C to T and G to A transitions at 5′ and 3′ fragment ends (Type II damage) (Günther and Nettelblad, 2019). These characteristics might influence mapping scores in low-coverage ancient genomes, particularly for those reconstructed from very short reads, eventually leading to an artificial decrement of reads carrying alternative alleles, in comparison to high-coverage modern genomes. In order to verify that this issue did not affect our downstream analyses, we compared the alternative allele frequency distributions between modern and ancient individual data. We used the PLINK 2.0 toolset to calculate the average proportion of alternative alleles for each individual. This analysis was repeated considering all SNPs, all SNPs without C to T and G to A and only transversions without finding significant differences between the pseudo-haploid datasets (derived from ancient and masked individuals).

Modern data preparation for analysis

The raw data were initially checked with Affymetrix suite software, then the data from 81 individuals that passed the quality control (call rate > 98.5) (Raveane et al., 2019) were converted into PLINK files and retained for the kinship analyses to exclude putatively related individuals using KING (Manichaikul et al., 2010). Considering that Indigenous populations have a higher degree of relatedness due to long periods of isolation and endogamy, there was the need to evaluate a different threshold. For this reason, the 97.5-percentile of population IBD for each population was used as threshold for exclusion (Busby et al., 2015). For each pair of related individuals, the exclusion was based on the number of missing SNPs. A total of 74 individuals (out of the initial 84) were retained after quality and kinship filters.

Ancient comparative datasets

The 545,942 SNPs retained in the rWD1560-dataset (see "Reduced worldwide (rWD1560) dataset" section) were called on the ancient dataset that contained our 12 ancient Panamanian individuals merged with 241 ancient Siberian and American individuals with a minimum coverage of 0.01X (Table S3). The calling was performed for all individuals in one run using ANGSD (Korneliussen et al., 2014) with the *haplocall 1* option, which picks a random read starting from an input set. In addition, to avoid possible biases due to low coverage data, we down-sampled all ancient genomes to 1X and 0.5X coverage using ANGSD with the *-downSample* option.

The ancient dataset was merged using PLINK 1.9 (Purcell et al., 2007) with our modern datasets and then filtered using–geno and–mind options set respectively to 0.60 and 0.98 (Scheib et al., 2018), keeping only individuals with at least 10,000 SNPs (Table S3) (Posth et al., 2018).

Modern comparative datasets

As detailed below, different comparative datasets were assembled: 1) a worldwide dataset of modern samples (rWD1560, 545,942 SNPs); 2) two datasets of (nearly) "unadmixed" Indigenous Americans (uIA217, 534,569 SNPs and uIA89 523,210 SNPs) obtained by removing individuals with signatures of non-Indigenous genetic contributions using different stringent criteria; and 3) a larger dataset of "admixed" individuals where only genetic fragments inherited from Indigenous individuals were retained, masking (removing) variants not belonging to haplotypes inherited by Indigenous groups (mIA417, 545,942 SNPs), to focus on pre-Hispanic interactions. The individuals used for the latter dataset were considered pseudo-haploid in allele frequency analyses, while in haplotype-based methods the individual chromosome pairs were jointly analyzed. Moreover, some of the samples with less than 50% Indigenous ancestry were removed (rmIA311).

1) Reduced worldwide (rWD1560) dataset

A first dataset of 4,939 modern individuals was built encompassing worldwide Affymetrix Human-Origins genotyped individuals and American whole-genome sequences from the literature considering a minimum threshold of 500K overlapping SNPs. This dataset

was merged using PLINK 1.9 with our modern individuals and then filtered using–geno and–mind options set to 0.02. After excluding related individuals (see "Modern data preparation for analysis" section), the dataset was geographically restricted to 1,560 individuals (rWD1560, Table S3) including our modern Panamanians (74), all individuals from America (1,084) and Siberia (203), and the western Eurasian (61), African (73) and Australasian (65) populations that left a greater genomic impact on Indigenous Americans during colonial times (Chacón-Duque et al., 2018; Homburger et al., 2015; Montinaro et al., 2015; Ongaro et al., 2019).

2) "Nearly unadmixed" Indigenous American (ulA217 and ulA89) datasets

European colonialism and the African slave trade left a strong impact on the Indigenous American populations. Therefore, the analyses of pre-colonial genetic history might be strongly influenced by these components and it is very difficult to find non-admixed modern individuals, even within Indigenous groups. Thus, three different approaches (ADMIXTURE, Local Ancestry and *f4*) have been used to create a sub-set of individuals with the maximum possible Indigenous genetic component, to avoid signals altered by recent admixture events. Considering the inconsistency of the preliminary results obtained by using the three methods independently, a stepwise merging approach was preferred, retaining individuals classified as Indigenous (with the lowest content of non-Indigenous component) after each step.

1. ADMIXTURE. We extend the analyses on our rWD1560 dataset until K20. However, considering that K14 has the lowest cross-validation (CV) error (Figure S2A), we used K14 to identify the individuals that have more than 95% of Indigenous components (290 in total) (Alexander et al., 2009).

2. f4 statistics. In the second approach, we used *f4* statistics in the following form: *f4* (ancientIndigenous, X; Europe/Africa, Mbuti). *Ancient Indigenous* was composed by five high-coverage ancient genomes selected on the basis of country of origin and age (Table S3). The selected individuals (N = 305) were those with a Z score < |3| for both Europe and Africa.

3. Local ancestry (LA). Combining the positive results of ADMIXTURE and *f4* statistics, we could retain 230 individuals to be selected for the Local Ancestry (LA) using the software RFMix (Maples et al., 2013). Among these, we selected 58 individuals to be used as ancestral source in LA analysis. The overall criteria used to select these 58 ancestral individuals were as follows: i) successfully passing the *f4* filter (see "*f4* statistics" section); ii) 100% IA in K14 (see "ADMIXTURE" section); iii) belonging to a population that best represents a specific IA component in the ADMIXTURE analysis (Figure S2A) for each K (until K20):

- K1 6 Puno individuals (selected at K20 among the population with more K1)
- K6 25 Guna individuals (selected at K14)
- K10 2 Chipewyan individuals (selected at K14)
- K11 10 Karitiana individuals (selected at K14)
- K17 8 Surui individuals (selected at K18)
- K20 7 Kichwa Orellana individuals (selected at K20)

We also used all African (73) and European (51) individuals (representing the respective ancestries). The Finns were excluded due to their known admixture with a central Asian population (Saag et al., 2019; Sikora et al., 2019). The entire dataset was screened for the LA of these selected individuals allowing us to identify 210 individuals showing less than 5% of non-IA ancestry (plus the 58 used as IA sources).

Merging all the positive results of these three independent analyses, we identified a restricted dataset with 217 almost unadmixed individuals (ulA217, Table S3). Moreover, more stringent criteria, i.e., < 1% African, < 2% European (Gnecchi-Ruscone et al., 2019) and Z < |2|, were used to select a second restricted dataset with only 89 almost unadmixed individuals (ulA89, Table S3).

3) Indigenous American dataset with masked haplotypes (mIA417)

The non-Indigenous component (> 5%) identified using LA was removed from each haplotype of the 417 individuals, not included in the almost unadmixed Indigenous dataset. This masked dataset mIA417 combined with ulA217 (or ulA89) creates an overall Indigenous dataset encompassing 634 (506) individuals.

Uniparental analyses

Ancient mitogenomes

Taking into account that the mitogenome sequence included in the whole hg19 human reference is different from the mtDNA reference sequence (rCRS) commonly used in phylogenetic studies on mtDNA, we have chosen rCRS for mapping the FASTQ data in our pipeline. Processed reads from shotgun (single-end) sequencing were aligned to the rCRS sequence (Andrews et al., 1999) with BWA v0.7.17 aln/samse algorithm (Li et al., 2009) and realigned with CircularMapper (Peltzer et al., 2016). Duplicate reads were removed with Picard MarkDuplicates (https://github.com/broadinstitute/picard) and BAM files were further processed with SAMtools (Li et al., 2009).

Raw paired-end reads derived from captured mitogenomes that overlapped for at least 11 bases were merged using ClipAndMerge v1.7.7 (Peltzer et al., 2016) and then processed as above (see "Ancient data preparation for analyses" section) with an additional step to remove the indexes used for multiplexing on the MiSeq sequencer. Clean reads were mapped to rCRS (Andrews et al., 1999) with BWA v0.7.17 mem algorithm and BAM files were filtered with Picard MarkDuplicates (https://github.com/broadinstitute/picard) to remove duplicates and with SAMtools (Li et al., 2009). The final mtDNA BAM of the four captured individuals were merged with the shotgun mtDNA BAM using SAMtools merge.

For all mitochondrial BAM files, only reads with minimum mapping and base quality of 30 and positions with a minimum depth of 1 were retained for downstream analyses. Eventually, we obtained 13 ancient mitogenomes with mtDNA genome coverage $\geq$ 0.99 (11 from pre- Hispanic individuals) (Table S1).

Two strategies were used to determine the haplotypes of these 13 mitogenomes. First, we performed variant calling with BCFtools (Li et al., 2009) and filtering the VCF files with VCFtools (Danecek et al., 2011). Haplotypes were refined by manually checking BAM files.

Then, to better define indels in our dataset, as there are diagnostic deletions for some Indigenous lineages, we realigned cleaned reads of our ancient individuals to modern Panamanian mitogenomes belonging to the same haplogroup. The alignment was performed with BWA 0.7.17 aln/samse algorithm (Li et al., 2009) and reads were realigned with CircularMapper (Peltzer et al., 2016). Consensus sequences were generated using the same filters as before and then compared to the rCRS to obtain final haplotypes.

We also reconstructed the consensus sequence for the four contaminated individuals. We used ANGSD (Korneliussen et al., 2014) applying the same filters as in Sánchez-Quinto et al. (2019).

Haplogroups classification, based on phylotree.org (mtDNA tree Build 17) (Van Oven, 2015), was assessed using the online tool HaploGrep2 (Weissensteiner et al., 2016).

Modern mitogenomes

After adaptors trimming paired-end reads were aligned to rCRS (Andrews et al., 1999) with BWA mem algorithm (Li et al., 2009). BAM files were filtered with Picard MarkDuplicates (https://github.com/broadinstitute/picard) and SAMtools (Li et al., 2009). Variant calling was performed with GATK HaplotypeCaller (McKenna et al., 2010) and mitochondrial haplotypes were also checked by manually inspecting BAM files. HaploGrep2 was used for haplogroup assignment (Table S1). We have also double-checked the final haplotypes for possible NUMTS without finding any problems. Four mitogenomes (PaGUN9659, PaGUN9671, PaNAS16050, and PaNGA1193) were obtained with Sanger sequencing and analyzed using Sequencher v5.0 (http://www.genecodes.com/).

MtDNA tree, dating, and demography

Phylogenetic tree and Bayesian Skyline Plot (BSP) were generated using BEAST v2.6.2 (Bouckaert et al., 2019). BEAST was also employed to calculate Bayesian age estimates. Radiocarbon dates of ancient individuals were used as priors. The L2c2 mitogenome from a Moreno individual (PaMOR16007) was included in the analyses as an outgroup. BEAST runs were performed with complete mtDNA sequences under the HKY substitution model (gamma-distributed rates plus invariant sites) with a fixed molecular clock as in (Brandini et al., 2018). We set the clock rate considering the ones published in Posth et al. (2016) and Soares et al. (2009). The chain length was established at 10,000,000 iterations with samples drawn every 1,000 Markov chain Monte Carlo (MCMC) steps, after a discarded burn-in of 10% steps (default value 0). Panama-specific haplogroups were set as monophyletic in the analyses. The same BEAST settings were used to: i) estimate the ages of haplogroups and (ii) evaluate population expansions in Panama through BSPs (Drummond et al., 2005) by including all Panamanian Indigenous mitogenomes analyzed in this study. BSPs were visualized in a plot using Tracer v1.7 (Rambaut et al., 2018) and converted into an excel graph by assuming a generation time of 25 years as in Brandini et al. (2018). The maximum clade credibility tree was determined using TreeAnnotator and visualized with FigTree (http://tree.bio.ed.ac.uk/software/figtree/).

Ancient Y chromosomes

The haplogroup classification of the eight ancient Y chromosomes (Table S1) was deducted from the aDNA aligned sequences by: i) extracting with bcftools all the positions belonging to the Y chromosome; ii) considering only the positions that matched the list of the SNPs belonging to the main branches of the phylogenetic tree present in Poznik (2016) after taking into account any possible aDNA damage (C/T–>T/C; G/A–>A/G) as in Fregel et al. (2018). To further sub-classify the ancient Y chromosomes the same workflow was performed by considering the list of 1,104 specific haplogroup Q SNPs reported by Grugni et al. (2019). All codes and pipeline for this part can be found at the link: https://github.com/raveancic/aDNAYchromosome.

Modern Y chromosomes

The Y chromosome haplogroup classification of the 43 modern male individuals was first inferred from genotyped files by using the script called Haplogroups.py in Yhaplo with Python3 (Poznik et al., 2016) (https://github.com/23andMe/yhaplo), using default parameters. Then, the obtained classification was confirmed by hierarchical analysis, as previously described (Battaglia et al., 2013), of the following Y chromosome haplogroup markers: M9, M242, M3, M89, YAP, M96, M304, M172, M241, M269, L23, S116. In addition, the M242 positive samples (Hg Q) were further sub-classified by typing the signature markers (M848, Z780, M925, Z5908, Y780, CTS2731) of the main Indigenous sub-haplogroups recently identified (Grugni et al., 2019; Pinotti et al., 2019). Haplogroup nomenclature is according to Grugni et al. (2019).

Population genetics analysis based on allele frequencies

Principal Component Analysis (PCA)

PCAs were performed using 'smartpca' program from the package EIGENSOFT v7.2.0 (Patterson et al., 2006). Ancient data, characterized by a large amount of missing data, were projected onto the modern variation with the lsqproject and autoshrink options. The same approach was used for the masked dataset (*mlA417)* that also shows a variable amount of missing data. Several PCAs were performed considering ancient and modern world-wide datasets and different sub-datasets. Those individuals showing peculiar outlier positions in the PCA plots were excluded from the downstream analyses (Tables S1 and S3).

ADMIXTURE clustering analysis

Different datasets (only modern and modern plus ancient individuals) were pruned with PLINK 1.9 (–indep-pairwise 200 25 0.4) and used to perform a biogeographical ancestry analysis with ADMIXTURE v.1.23 (Alexander et al., 2009). We performed ten independent unsupervised ADMIXTURE runs for each K, from K1 to K20, adding the –cv flag to identify the 5-fold cross-validation (CV) error for each K. The average cross-validation (cv) value for each K were plotted to select the model with highest likelihood. The software CLUMPAK (Kopelman et al., 2015) was used to combine different runs and to find the best alignment of the results across a range of K values with the tool DISTRUCT (Rosenberg, 2004).

The analysis on the rWD1560 dataset reveals well-defined structures and consistent trends, associated with a low CV value, until K14 (or even K20) suggesting that the observed pattern is not an artifact. In the ADMIXTURE plot it is possible to observe seven specific IA ancestries, some mirroring the PCA clusters (Figure 2B):

- K1 that is widely distributed in all IA populations with high percentage in Puno, Aymara, Quechua and Paran-Cusco individuals, all speaking Andean languages.
- K6 is modal in the Guna and highly represented in all the populations from Costa Rica to Panama, speaking Chibchan languages.
- K10 is typical of the Chipewyan (speaking a Na-Dene language) with lower percentage in all populations from northern North America.
- K11 is modal in Karitiana and Surui speaking Tupi (Equatorial-Tucanoan) languages.
- K17 separates the Surui from Karitiana.
- K15 is represented by the Pima and mostly present in Mexico, but also widely distributed in Central and Northern IA speaking groups.
- K19, like K1, is widely distributed across the double continent and reaches the highest level in South America, particularly in the Andes Mountains (i.e., KCH).

Additional interesting components are K13 and K16 that are present in high percentages in Puerto Rico (PUR) and Colombia (CLM), respectively. They also can be observed in admixed American and European populations. The above-mentioned components are present in different proportions and differentially distributed among IA populations including the Panamanians, with the only notable exception of the Guna showing a specific component. The addition of 329 ancient Siberian and American individuals to the rWD1560 dataset confirms the already-discussed ancestries, revealing an additional K specific of Archaic Caribbean individuals (Figure 2A). A further ADMIXTURE analysis (Figure S2B) was performed projecting the ancient individuals on to the population structure from only modern individuals using the option *-P* and the *.P* file from the analysis in Figure S2A at K14.

Admixture tests (f statistics)

The *f* statistics was performed using EIGENSOFT v7.2 and AdmixTools v4.1 (Patterson et al., 2012). Outgroup *f3* was used to highlight only the shared genetic history between individuals or populations relative to an outgroup (Peter, 2016). A high *f3* value means more genetic history shared between the pair population analyzed. This method is less sensitive to lineage-specific genetic drift over the use of pairwise distance measures, such as *Fst* (Skoglund et al., 2015). A graphic explanation of the outgroup *f3* is reported in Figure S3.

We analyzed the shared genetic history of modern IA populations (included in the mIA417 and uIA89 datasets) against some ancient reference genomes (aRG) from Siberia, Beringia, North America (representative of the NNA ancestry) and South America (representative of SNA). The Guna always show a shared genetic drift with the ancient reference individuals lower than the average *f3* value (dotted line) of all modern IA groups. It could be also noticed that the average *f3* value is higher in the comparison with Spirit Cave than with Anzick-1.

We also built a distance matrix using the inverse values derived from the outgroup *f3* statistics on all Central and South American populations pairs plus Anzick-1, Early San Nicolas (ESN), Spirit Cave and USR-1 (as an outgroup). We retained only populations with more than 30K overlapping SNPs and significant Z scores (p value$\sim$0.001, for Z scores > |3.3|) in all comparisons. This distance matrix was used to generate a neighbor joining tree (Figure S3C) with the program PHYLIP 3.6 (Nägele et al., 2020). The tree was visualized with FigTree 1.4.4 (https://github.com/rambaut/figtree).

The *f4* statistics was eventually used to identify gene flows among different populations. The comparison was performed in the form *f4(W, X; Y/test, Outgroup),* as reported in the software documentation. A graphic explanation of the *f4* statistics analyses is reported in Figure S5. In each figure showing a *f4* statistics test the form is reported above the plot(s). Results from *f4* analyses presented in Figure 2C display only tests in which the initial conformation of the tree is rejected (p$\sim$0.001, Z score > 3.3 or < −3.3) (Moreno-Mayar et al., 2018), meaning that the investigated population (Y) has a significantly higher genetic affinity with W rather than with X if the *f4* results are positive, the opposite when values are negative. If the results are not displayed, the proposed tree cannot be rejected and there are no significant preferential relationships between the test population (Y) and W or X. In Figure S5 the Z score is displayed in abscissa and the region where the tested tree cannot be rejected is highlighted in gray (see above).

In all *f4* statistics, we considered a minimum threshold of 30K SNPs, the comparisons with less SNPs are highlighted with a specific symbol (X). Due to the low number of SNPs retained in multiple analyses, the following individuals were excluded: Baja_100, CuevadelPerico_2700, Enoque_3500, Kaillachuro_4000, LosIndios_600, Moraes_5800, SanFranciscoBay_25, ShukaKaa_10300, SoroMikayaPatjxa_6800 and Tibes_1200.

In particular, to specifically check for the relationships between Anzick-1 and Spirit Cave, with the Isthmian populations as well as with other ancient and modern IA individuals from Central and South America, we ran two *f4*statistics in the following forms *f4* (Anzick-1, Spirit Cave; Isthmo, Mbuti) and *f4* (Anzick-1, Spirit Cave; Central and South IA, Mbuti). The datasets uIA89, mIA417 and ancient individuals were used considering different sets of variants: all SNPs, all SNPs without C to T and G to A variants, only transversions and only transversion with ancient individuals' coverage downsampled to a maximum of 1X (to avoid coverage biases).

We observed a clear pattern that becomes significant when increasing the number of SNPs. We further verified this pattern using a *f4* statistics in the form *f4* (USR-1, Anzick-1/Spirit Cave; Central and South IA, Mbuti) that confirmed a higher proximity to Spirit Cave in comparison to Anzick-1. The same pattern has been also observed in the outgroup *f3* analyses (see above).

TreeMix

In order to obtain a maximum likelihood tree, we ran TreeMix (Pickrell and Pritchard, 2012) on the pruned dataset uIA89 using TSI, CHB and YRI (Tuscans, Chinese Han and Yoruba) as outgroups. The -noss and -global parameters were added considering zero to five admixture edges. The trees with the highest likelihood were selected after 1,000 runs (Gnecchi-Ruscone et al., 2019; Moreno-Mayar et al., 2018).

Ancestry modeling with qpWave

In order to verify that the Isthmo-Colombian ancestry (UPopI) is independent from other IA ancestries, we compared in pairs the Isthmian populations with all other modern and ancient IA populations using *qpWave* (Patterson et al., 2012) to test whether they were homogeneously related to a set of external outgroups. The outgroups were kept to the minimum and chosen to represent different IA ancestries identified here and in other papers:

- Mbuti, Papuan, CHB, Malta_24000 and USR-1_11500 as non-IA sources (Nägele et al., 2020; Posth et al., 2018)
- ASO_4000 and Chipewyan for NNA
- LagoaSanta_10400 for SNA1
- SpiritCave_10900 for SNA2
- Mixe for UPopA
- GuayaboBlanco_1700 for Archaic Caribbean
- Ayayema_4500 for Patagonia
- Aymara and KCH (K1 and K19 respectively in Figure S2A) representing modern South American populations.

We took in consideration the p value of "*taildiff*" for Rank1, a statistically significant p value (< 0.01) means that each compared pair could be explained by two sources. We observed that one ancestry is usually needed (p value > 0.01) to define pairs of Isthmo-Colombian populations, while pairs of Isthmian and non-Isthmian populations require two ancestries. This pattern is more evident in the Guna, the best representative of the Isthmo-Colombian component. This pattern confirms that a different ancestry, instead of only genetic drift by isolation, is needed to explain the distinctiveness of the Isthmo-Colombian populations.

Demographic modeling with qpGraph

We used *qpGraph* (Patterson et al., 2012), on a merged dataset of the uIA89, mIA417 and ancient individuals (considering only transversions), to reconstruct the best tree modeling the relationships between Isthmian populations and ancient Indigenous genomes. In our *f4* statistics we noted a differential relationship between Isthmian groups and modern/ancient Indigenous Americans in comparison to the individuals older than 10 kya (Figure 6A; Table S4). Therefore, we modeled a basal tree with three of the most ancient available genomes of the SNA ancestry, an ancestry that certainly went through the Isthmus to reach South America. Our best tree revealed that the SNA dispersal involved a complex demographic pattern, with three possible ancestries (Figure S6A). To resolve the inferred zero-length internal branch, we tested all three possible split orders obtaining similar scores. Therefore, it might represent a very short branch that we cannot resolve with this dataset power (Lipson, 2020) and the three lineages, Anzick-1 (Montana, ~12.6 kya), Lagoa Santa (Brazil, ~10.4 kya; SNA1) and Spirit Cave (Nevada, ~10.9 kya; SNA2) are statistically consistent with forming a trifurcation. The best fitting topology was tested by considering an early admixture between the SNA2 source and SNA1 obtaining a still supported model without zero-length branches (Figure S6B). To increase the resolution power and considering the results of previous analyses (*f3*- and *f4*-statistics), we added to this graph the captured and genotyped data from Lapa do Santos (Brazil, ~9.6 kya) as SNA1 and the whole-genome sequences of ESN (California; ~4-5 kya) as SNA2. This allowed us also to check for any bias due to sequencing methods. Even in this case the best fit tree confirms the trifurcation (Figure S6C). After this step, we added Los Rieles (Chile, ~10.9 kya), the most ancient Pacific coast genome, which turned out to be better modeled as an admixture of SNA1 and SNA2 ($|Z| = 2.835$) than as non-admixed and considering only geographic origins ($|Z| = 3.930$) (Figure S6D). This finding confirms that both SNA1 and SNA2 reached South America and seems to indicate that the latter had a lower impact on the Atlantic side of South America. When Los Rieles is replaced by Lapa do Santos, the tree does not fit ($|Z| = 3.930$) (Figure S6E).

We then took into account that, in the *f4* statistics (Figure 6A; Table S4), there is a significant allele sharing of the Isthmian populations with Spirit Cave and two Central American ancient genomes, Mayahak Cab Pek (Belize, ~9.3 kya) and Saki Tzul (Belize, ~7.4

kya), as well as a higher genetic proximity to Los Rieles relative to Lagoa Santa. Therefore, we attempted to model ancient Panama in relation to these ancient genomes (Figures S6F and S6G). Ancient Panama fits better when considering an admixture between the Central-South American branch of SNA2 and another ancestry parallel to SNA2 and shows the best score with Mayahak Cab Pek (Figure S6G). The additions of NNA individuals (Figure S6H), ASO (Ancient Southwestern Ontario, ~4.2 kya), 939 (Lucy Island, British Columbia, ~6.1 kya), Kennewick (Washington State, ~8.8 kya), ancient Athabaskan (dated 100 and 725 ya), and modern Chipewyan, hold better when assuming some admixture events involving these genomes. These findings confirm that we cannot identify an unadmixed proxy for the NNA ancestry among ancient individuals. The best graph was obtained when including ASO as NNA and Mayahak Cab Pek as the central American ancient genome.

At this point, we further evaluated the relationship of Panama with SNA1 that we initially linked to Lagoa Santa (Figure S6A). As before, we started from basal admixture graphs without Guna and considered the conformation with ASO and Mayahak Cab Pek, based on previous results (Figure S6H). We first tested the tree without admixture in Los Rieles, placing Lagoa Santa as a parallel branch of SNA2, but the tree would fit only when considering Los Rieles as an admixture between SNA1 and SNA2 ($|Z| = 2.896$), the two early South American ancestries that we identified above (Figure S7A). It is worth mentioning, however, that the graph without admixture in Los Rieles became statistically significant ($|Z| < 3$) when Lagoa Santa was replaced with the younger Laranjal sample (Brazil, ~6.8 kya) (Figure S7B). This confirms our *f4* statistics (Figure 6A; Table S4) and the scenario of a widespread population turnover in South American during mid-Holocene, as previously suggested (Moreno-Mayar et al., 2018; Posth et al., 2018), a finding that also correlates with climate changes in the southern continent (Riris and Arroyo-Kalin, 2019). As for the Ancient Panamanians, they are a mix between the source of SNA2 (prior to Spirit Cave) and the admixture between SNA1 and SNA2 (Figure S7A).

Lastly, we assessed different admixture graphs also including the Guna, which was the best representative of the Isthmian-specific component in our previous analyses (Figure 2A). As for the ancient Isthmians, we first explored the link of Guna with SNA2 (i.e., Spirit Cave) and in this setting only the admixed model was supported, with the Guna group representing a still unsampled population of the Isthmus, UPopI (Figure S7B). To assess if UPopI might correspond to the previously identified UPopA, we replaced Guna with Mixe, previously used to identify UPopA (Moreno-Mayar et al., 2018). The resulting admixture graph was not statistically supported ($|Z| > 3$, the rightmost graph). Then, we linked Guna also to SNA1, obtaining the best Z score in the graph when UPopI was placed as a parallel ancestry to SNA1 and SNA2, all radiating from the same early SNA source (Figure S7C). The latter derives from an initial split of the early Indigenous group into SNA and NNA. In this scenario the ASO group is the result of an admixture between NNA and SNA1. It is therefore likely that the first split occurred further north and earlier than the diversification of SNA into SNA1 e SNA2. Finally, the same graph shows that when UPopI reached the Isthmian area, it admixed locally with population groups derived from both SNA1 and SNA2.

Taking into account the presence of a zero-length internal branch in the final tree with UPopI (Figure S7C) and the results obtained on the basal graph (Figure S6), we modeled a binary tree without zero-length branches when considering an initial migration of population with an early SNA ancestry (SNA1) and a later North American admixture between SNA1 and a different SNA branch (SNA2) (Figure 7). This admixture gave rise to two ancestries, one, related to Spirit Cave, that reached South America, leaving evident footprints on the Pacific coast, and another restricted to the Isthmo-Colombian area (UPopI) that is well represented in the Guna. The best topologies were also checked replacing Guna (UPopI) with Mixe (UPopA), Spirit Cave with Anzick-1, and without UPopI (Figures S7D–S7F), but no statistically supported graphs were found. The other Isthmian Indigenous groups were also tested (replacing ancient Isthmians) using this final model (Z score always < 2.5) to estimate the differential legacy of the three ancestries in present-day populations (inset of Figure 7).

Population genetics analysis based on reconstructed haplotypes

Phasing

Phased haplotypes were generated from the rWD1560 dataset using the Segmented Haplotype Estimation and Imputation tool SHAPEITv2 (Delaneau et al., 2011) and the HapMap37 human genome build 37 recombination map.

Local Ancestry and Masking

The local ancestry for genomic fragments in the American individuals was estimated using RFMix (Maples et al., 2013). As source populations, we used Bantu, Esan (ESN), Gambia (GWDwg), Mandenka, Mbuti and Yoruba (YRI) for Africa, Spanish (IBS), British (GBR), French, Icelandic and Tuscany (TSI) for Europe and Chipewyan, Kichwa Orellana, PaGUNA, Puno, Surui and Karitiana for Indigenous ancestry. We used "PopPhased," "-n 5" and "–forward-backward" options as recommended in RFMix manual. Then, starting from RFMix output files, we built a PLINK file set in which the non-Indigenous SNPs were masked. The masking process was done with this rationale: if in the "Viterbi" output a particular SNP was not assigned to the Indigenous ancestry and if the probability of belonging to the Indigenous ancestry (reported in the "forwardbackward" output) was less than a threshold (< 0.9) that allele was set as missing. In this analysis we kept individuals as separated into the two phased haplotypes.

ChromoPainter

To obtain the painting profile of all the 217 individuals in the ulA217 dataset consisting in a matrix of 'recipient' individuals (rows) that appear as a mosaic of the 'donors' (columns), we processed the genomic information contained in phased data (haplotypes) through the use of inferential algorithms implemented in CHROMOPAINTERv2 (Lawson et al., 2012). Technically for this analysis the recombination (-n) and mutation (-m) parameters used were respectively 233.1352 and 0.00084 estimated on five randomly selected

chromosomes (3, 7, 10, 18 and 22). Since the genetic variability among IA populations is low, we ran CHROMOPAINTER in two runs, one with standard parameters, the other adding the flag -k 50 (Gnecchi-Ruscone et al., 2019). No significant differences were observed between the two runs.

fineSTRUCTURE

The CHROMOPAINTER square (217 × 217 individuals) *chunkcounts.out* matrix was used as input file for fineSTRUCTURE in order to identify similar genetic clusters. We ran the software with three millions MCMC iterations thinned every 10,000 and preceded by one million burn in iterations: -x 1000000 ; -y 3000000 ; -z 10000 ; -t 1000000. The MCMC file (.xml) was used to build the tree structure using both the options –T1 and –T3, without major changes between the two methods.

Initially, we obtained 50 clusters in the final tree (data not shown). However, to obtain more robust genetic inferences the number of clusters was reduced to 19 considering the number of individuals in each cluster (less than five) and the Total Variation Distance (TVD < 0.03) as elimination criteria. TVD is an index that measures the similarity between copying vectors of the CHROMOPAINTER matrix (calculated on the chunklengths) (Leslie et al., 2015); lower values of TVD mean similarity, while higher values indicate heterogeneity.

Haplotype Analyses on 'Masked' Individuals

The masked haplotypes (mIA417) were initially filtered for the individuals that had a maximum of 50% of missing SNPs (considered as the mean of the summed missingness of the two haplotypes) and, among these individuals, we selected only those with at least 25% of SNPs retained in each haplotype. Eventually, we obtained a restricted dataset of 311 masked individuals (rmIA311). This dataset (rmIA311) was then converted in PLINK1.9 format and subsequently in a CHROMOPAINTERv2 input. To enable missing data in CHROMOPAINTERv2, we slightly modified CHROMOPAINTERv2 such that a recipient/target's emission probability is set to 0 at missing (i.e., masked) SNPs when tabulating the expected number of segments matched to each "Donor" individual that the recipient is compared to. Therefore, in regions of high missingness the expected number of segments matched to each "Donor" will tend toward the prior, which assumes equal matching to all "Donor" individuals. However, in our application here we found that inference seems to be dominated by data at non-missing SNPs, where the usual CHROMOPAINTERv2 machinery is employed. In particular, we did not identify any correlation between the percentage of missing data (even when reaching 50%) and bad placements/outlier behaviors in the PCA created from the CHROMOPAINTER output projecting the 'masked' individuals (Figure S4A).

Identical by Descent (IBD) Analysis

The pattern of IBD sharing within each population of the uIA217 phased dataset was analyzed using Refined-IBD (Browning and Browning, 2013), which makes it possible to improve the accuracy and efficiency of identity by descent detection in population data, using default parameters. The average IBD-sharing was calculated for nine different bin categories corresponding to different degrees of relatedness (Gnecchi-Ruscone et al., 2019; Moreno Estrada et al., 2014). The total length of shared IBD was calculated for each bin, by considering all pairs of individuals within each population group. The summed length was then divided by the numbers of pairs in each population in order to obtain the average total length of intrapopulation IBD shared blocks for each population in the uIA217 dataset (y axis in Figure 3C).

In order to reconstruct the population dynamics, we applied IBDne on the uIA217 dataset, using both IBDseq, which does not require phased data, and Refined-IBD that uses phased data, using different minimum thresholds of IBD segment length (2 and 4 centimorgan, cM). Considering all the Panamanian individuals, lower confidence intervals were obtained when using windows of 2 cM. Moreover, the Ne obtained with Refined-IBD is more compatible with historical estimates of the area's pre-colonial population size (see introduction). We observed the same trend in the ancestry-specific effective population size (asIBDne) from the 74 Panamanian individuals, masked for the IA component, following the pipeline presented by Browning et al. (2018), as reported in Ongaro et al. (2019). Therefore, Refined-IBD was applied using 2 cM windows for the comparison between Panamanian and non-Panamanian IA individuals present in the uIA217 dataset (inset Figure 3C). This analysis shows a decrease in the region's population size that pre-dates the average values of other IA populations considered together. This decrease started in pre-Hispanic times (~1100 ya) then became steeper in the early colonial period (~500 ya). To retain more information, we used the three macro-clusters from the fineSTRUCTURE tree: Guna (30 individuals), Emberá (18 individuals) and Western Panama (20 individuals) encompassing Bribri, Naso and Ngäbe. The Guna group shows a peculiar trend when considering shorter IBD fragments < 6 cM (Figure S4C). However, even when the Guna were removed from the Panamanian / non-Panamanian comparison, the peculiar pre-Hispanic demographic contraction of the Panamanian populations was still detectable and with smaller confidence intervals (Figure S4D). The same approach was applied including all of the macro-clusters obtained with fineSTRUCTURE and considering a minimum threshold of 8 cM. This analysis confirmed the behavior of the Isthmian groups including the Guna (Figure S4E).

Dating Admixture Events with IBD Sharing

In order to date the admixture events between our Panamanian groups and other IA populations included in the uIA217 dataset, we calculated the IBD sharing segments using RefineIBD as performed by Liu et al. (2020). The IBD blocks were divided into three categories, based on their length (1-5 cM, 5-10 cM and over 10 cM), each roughly representing different time periods: 1,500-2,500 ya, 500-1,500 ya and < 500 ya (Liu et al., 2020; Ralph and Coop, 2013). We have calculated the mean of summed IBD lengths shared between population pairs for each length category. To reduce noise and false positives only the pairs that shared at least two blocks > 5 cM and four < 5 cM were considered.

ADDITIONAL NOTES

The text has been revised in order to minimize the use of ''colonial language'' and to avoid the connotation of people as mere samples or data. The adjective Indigenous has been preferred to Native American with only notable exceptions of Northern Native American (NNA) and Southern Native American (SNA) ancestries, which were used for consistency with previous papers.

Many figures in the paper have been created using various versions of the software Tableau (https://www.tableau.com/) or with different R packages.

CellPress
OPEN ACCESS

Supplemental figures

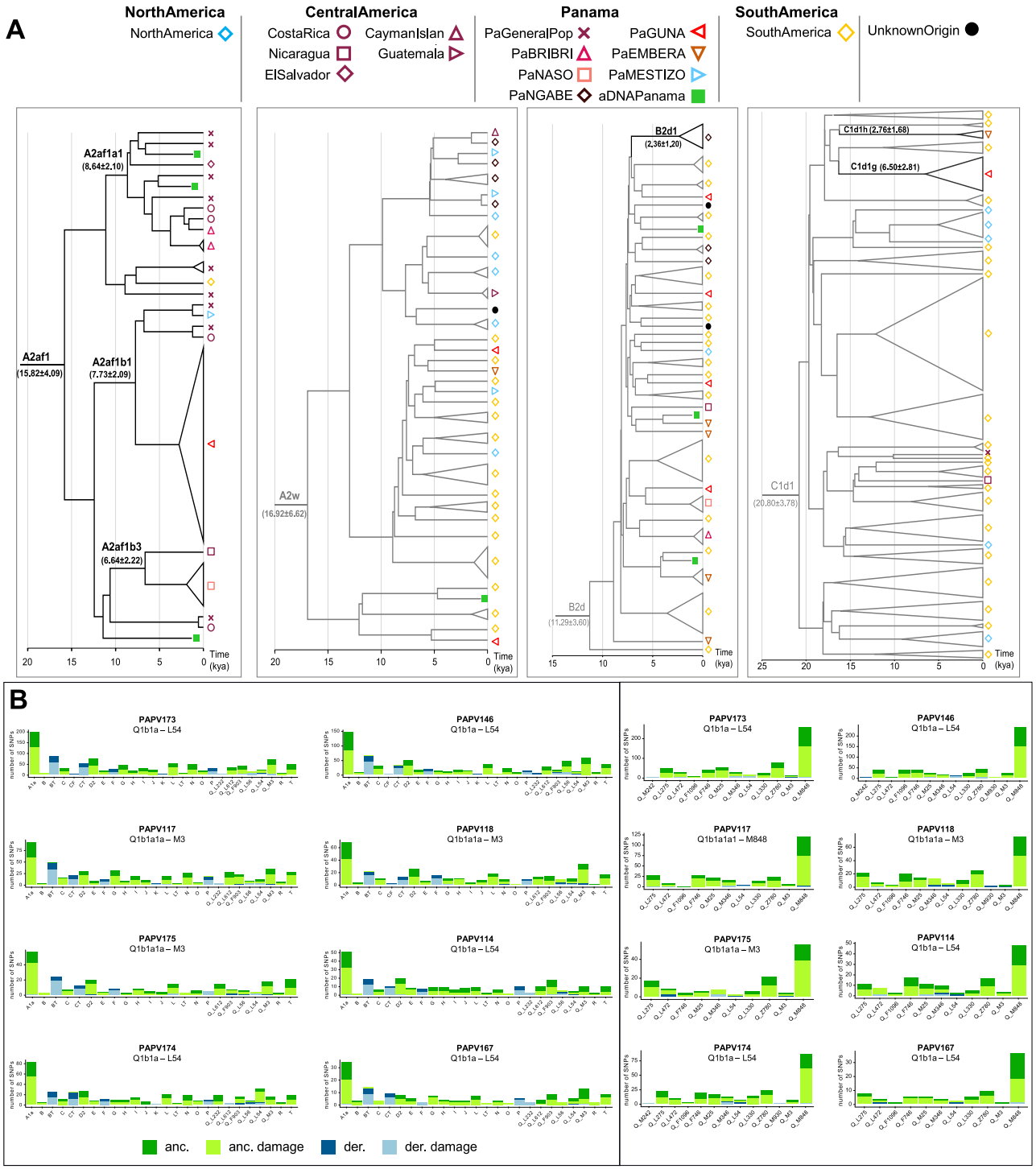

(legend on next page)

Figure S1. Analyses of uniparental markers, related to Figure 5B and Table S1

(**A**) Schematic phylogenetic trees of the four major mtDNA haplogroups identified in the Isthmian area. The Bayesian phylogenetic trees, rooted on an L2c2 mitogenome from a "Moreno" individual, include all modern mitogenomes belonging to the four major haplogroups of modern and ancient Isthmian individuals (A2af1, A2w, B2d, C1d1). Black lines highlight branches specific to IA from the Isthmo-Colombian area. The Bayesian age (mean value with standard deviation) is shown for relevant branches. (**B**) Ancient Y chromosome classification. SNPs for each macro-haplogroup present in Poznik et al., 2016. In the right panel, SNPs for each sub-haplogroup Q in Grugni et al., 2019 and Pinotti et al., 2019. Different colors refer to the allele status (green: ancestral; blue: derived), while different shades indicate the aDNA possible damage. Haplogroup nomenclature as in ISOGG 2019.

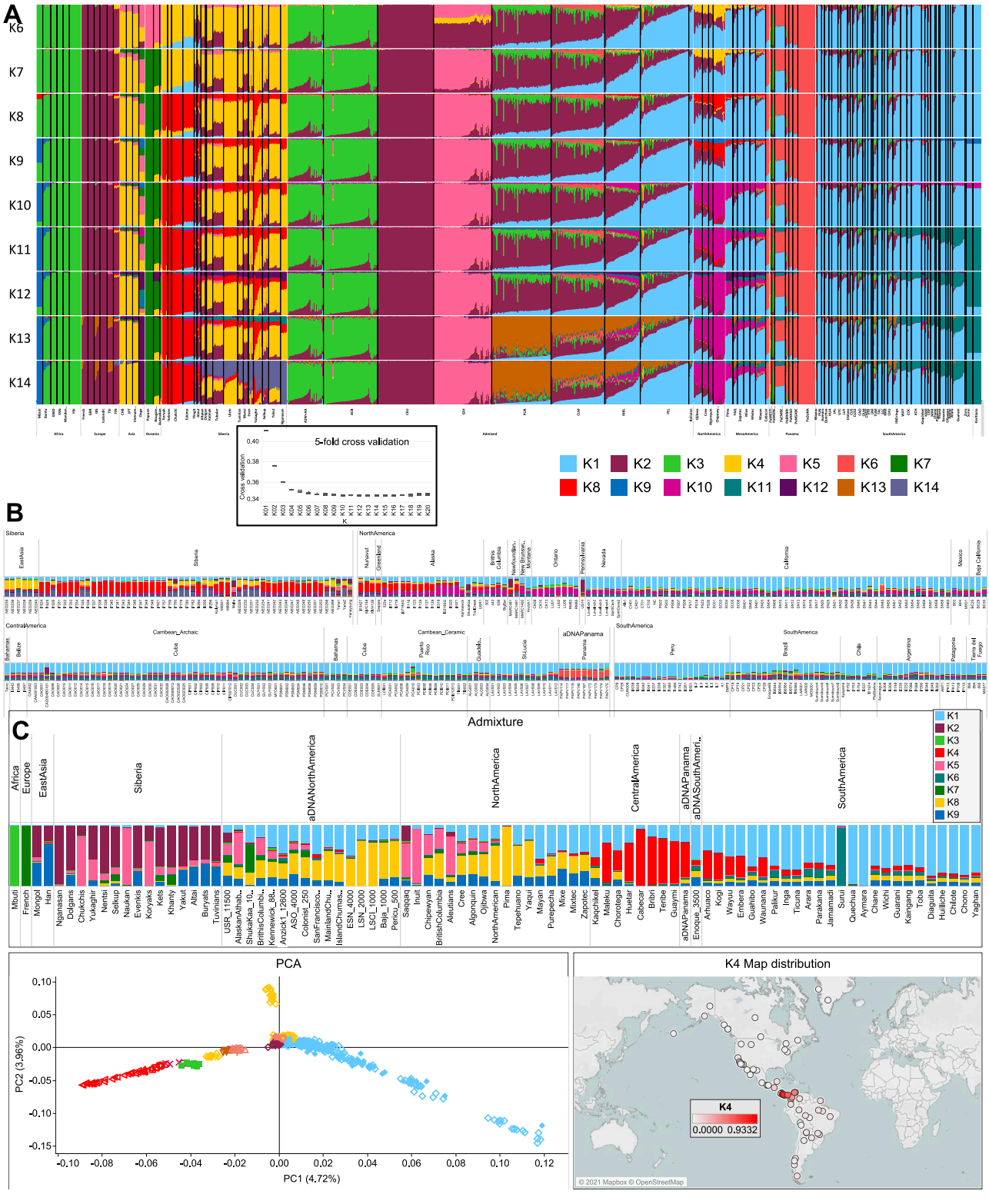

(legend on next page)

Figure S2. Worldwide ADMIXTURE plot on modern and ancient individuals, related to Figure 2

(**A**) ADMIXTURE analyses were performed from K1 to K20 on the modern rWD1560 dataset, even if only profiles from K6 to K14 are displayed. The inset shows the boxplot of 5-fold cross validation (CV) values for Ks from 1 to 20 after 10 runs. The median (most typical) values were plotted indicating 25th and 75th percentiles (dark and light gray, respectively) and arms extending 1.5 times the IQR (interquartile range). (**B**) ADMIXTURE analysis projecting ancient Siberian and American individuals on the modern worldwide variability. (**C**) ADMIXTURE plot and PCA performed on a comparative dataset (genotyped with Illumina chips) from Scheib et al., 2018 that includes the following Chibchan-speaking populations: Arhuaco and Kogi from Colombia; Guaymi, Cabecar, Teribe, Bribri, Huetar and Maleku from Costa Rica (Table S3). The K4 distribution map is also shown.

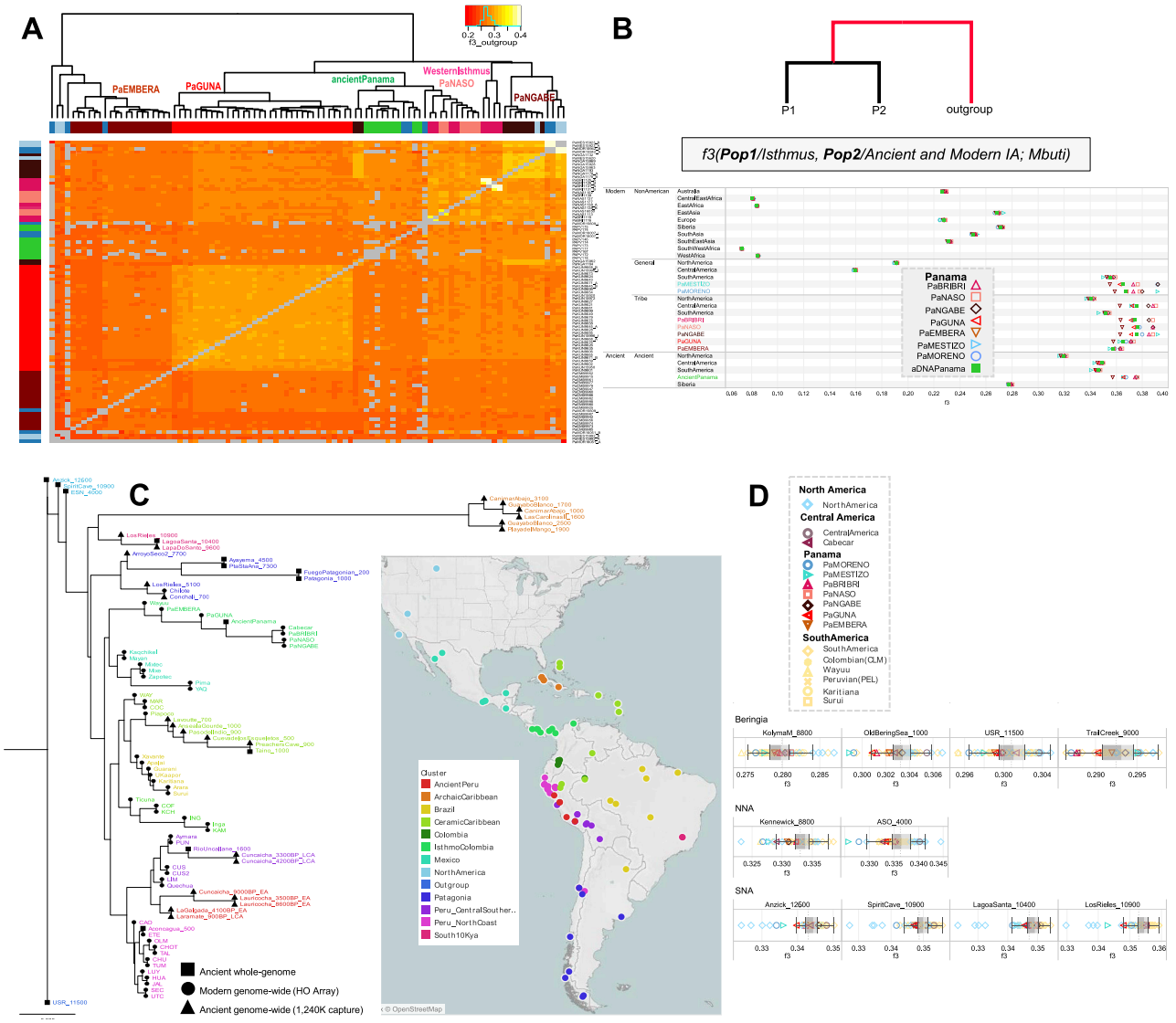

Figure S3. ***f3*** **statistics involving Isthmian individuals, related to Figures 2, 3, and 6**

(**A**) Heatmap based on outgroup *f3*-statistics. The shared drift among the Panamanian individuals was analyzed considering those included in uIA217 plus ancient individuals and masked data in mIA417. Color intensity is inversely proportional to the shared ancestry among individuals, which was used to build the dendrogram. (**B**) Outgroup *f3* statistics where ancient and modern Isthmian groups (Pop1) were compared to worldwide populations (Pop2) including non-American groups in the rWD1560 dataset, all populations in the mIA417 and uIA217 datasets and all ancient individuals. All comparisons have a Z score > 32.912. The average *f3* value for each population is reported in abscissa. (**C**) The neighbor-joining tree is built using the inverse values derived from the outgroup *f3* statistics on all Central and South American populations pairs plus Anzick-1, Early San Nicolas (ESN), Spirit Cave and USR-1. The latter is considered as an outgroup in the tree. We retained only populations with more than 30K overlapping SNPs and significant Z scores (> 3.3) in all comparisons. The map shows the geographic distribution of the populations, which are colored according to their genetic proximity in the tree. (**D**) We also analyzed the shared genetic history of modern IA populations (included in mIA417 and uIA89) against ancient reference genomes from Beringia and the Americas (representative of the NNA and SNA ancestries). Boxplots in gray help to visualize the distribution of *f3* values in each comparison, indicating the median (most typical) value, 25th and 75th percentiles (dark and light gray, respectively), and arms extending 1.5 times the IQR (interquartile range). The dotted line indicates the *f3* average value.

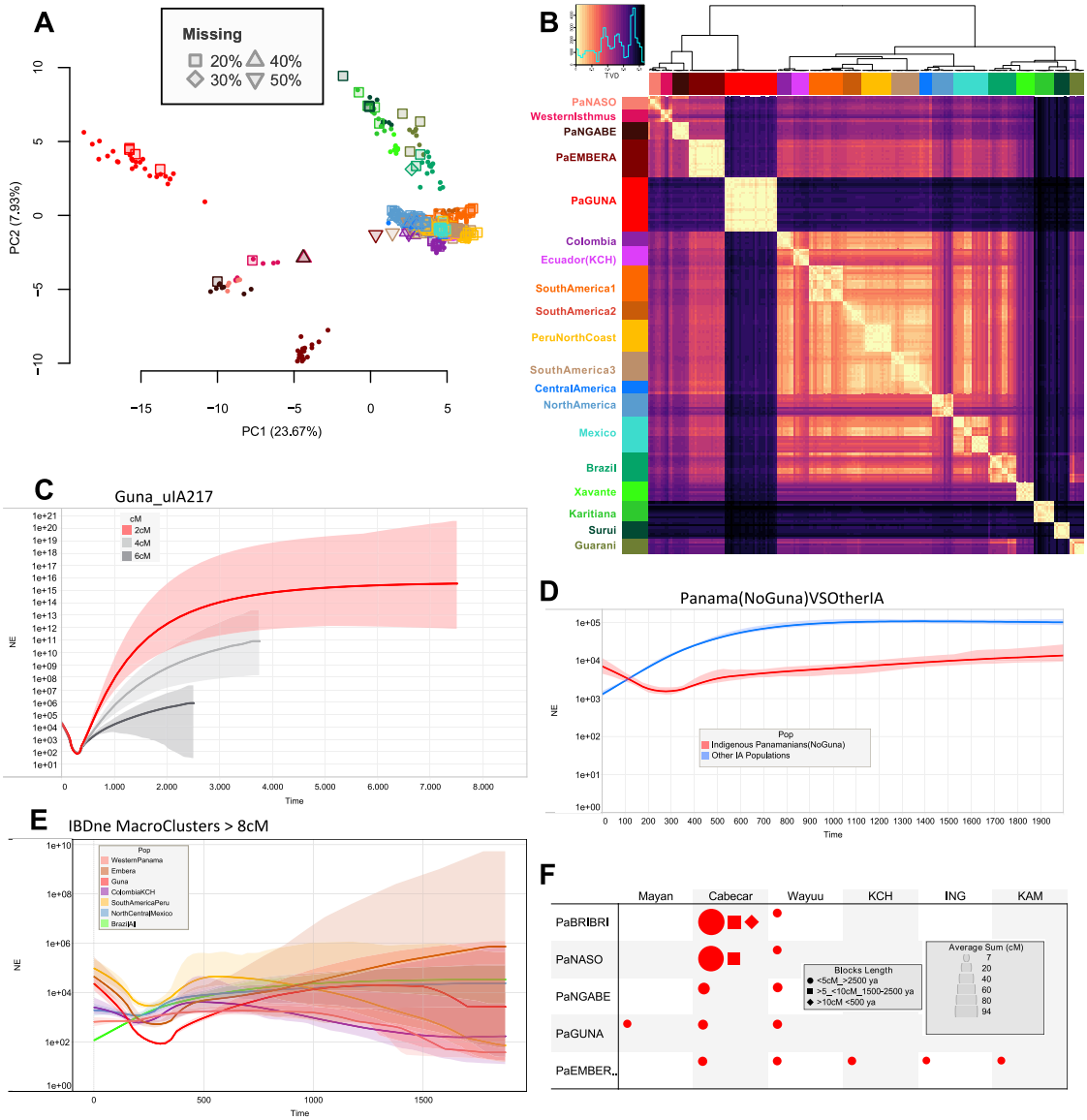

Figure S4. Haplotype-based analyses and estimates of effective population size variation over time, related to Figure 3

(**A**) The PCA was built using copying vectors inferred using a modified version of ChromoPainter that allows for the presence of missing data. The masked individuals (rmIA311) have been projected on the variability of the nearly unadmixed individuals (ulA217) regardless of the level of missing data. The unadmixed individuals are indicated with full filled dots while the masked ones are represented by different shapes, according to the percentage of missing SNPs. The colors refer to the clusters (donors) of Figure 3A. (**B**) Heatmap based on individual TVD (Total Variation Distance) values. Dendrogram branches are colored according to 19 clusters (Figure 3A). The TVD was compared both among and within clusters. Lighter colors (lower TVD values) in the matrix mean similarity, while darker colors (higher TVD values) indicate heterogeneity.

(**C**) We used RefinedIBD on inferred IBD length to estimate variations in the effective population size (Ne, on a log scale y axis) over time. The x-axes show the time before the present as years ago (ya) considering a generation time of 25 years and the colored regions show 95% bootstrap confidence intervals (CI). The analyses were limited to the last ~2,000 years, due to the wide variance of exponentially distributed IBD fragments and were performed on different datasets. The Guna group was evaluated considering different IBD thresholds (2 cM, 4 cM and 6 cM). (**D**) We double-checked the trend presented in the inset of Figure 3C without the Guna. (**E**) We also compared the IBDne of the Panamanian macro-clusters with the others identified in Figure 3A, Western Panama: Western Isthmus, PaNASO, PaNGABE; Emberà: PaEMBERA; Guna: PaGUNA; Colombia KCH: Colombia, Ecuador (KCH); South America Peru: SouthAmerica1, SouthAmerica2, Peru North Coast, SouthAmerica3; North Central Mexico: Central America, North America, Mexico; Brazil all: Brazil, Xavante, Karitiana, Surui, Guarani. (**F**) Visualization of the average of summed IBD lengths shared between modern Panamanians and other IA populations in each paired comparison, with identified IBD blocks in the range of 1–5 cM (oldest), 5–10 cM, and over 10 cM (youngest). Shape sizes are proportional to mean values; only those pairs sharing at least two blocks > 5 cM and four < 5 cM are plotted.

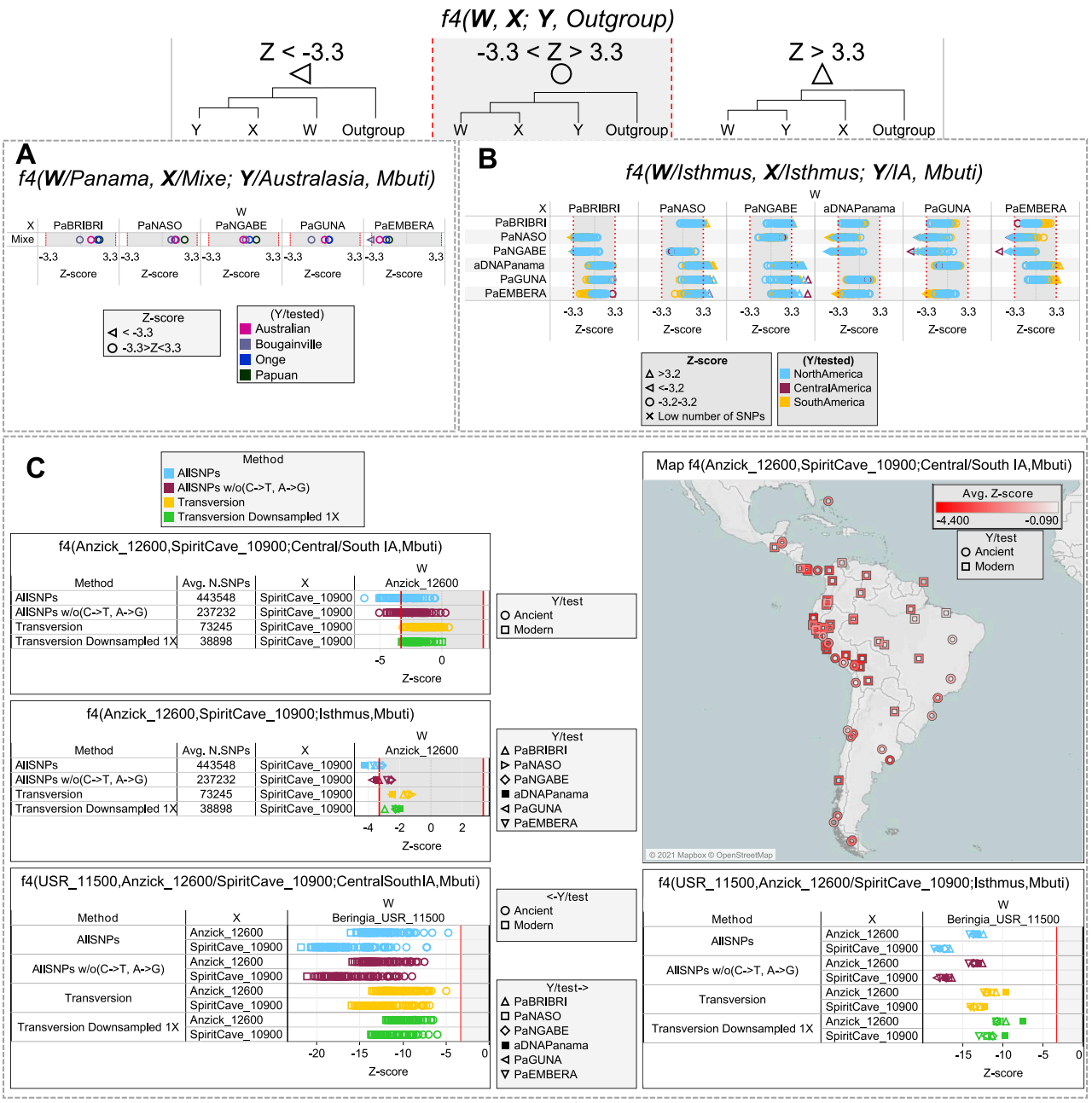

Figure S5. ***f4*** **statistics involving Isthmian individuals, related to Figures 2 and 4**

(**A**) *f4* statistics in which Panamanian populations (W) were compared to Mixe (X), typically used to reveal UPopY among IA, and to four Australasian populations (Y). (**B**) Isthmian groups (W) were compared to each other (X) testing for other IA populations (Y, colored according to their geographic location) to test through the Z score whether a given Isthmian group carries excess of a specific IA ancestry. (**C**) To specifically test the differential relationships of Isthmian and other Central/South IA groups with Anzick-1 and Spirit Cave, we ran the *f4* -statistics in the form *f4* (Anzick1, Spirit Cave; Central and South IA, Mbuti) and reported the average Z score on a map. The Isthmian populations were also tested separately. In the lower part of the panel, we verified the same relationships in the form *f4* (USR, Anzick1/Spirit Cave; Central and South IA, Mbuti), using USR as outgroup to the Central and South IA populations (again the Isthmian populations were tested separately, plot on the lower right). The datasets ulA89, mIA417 and ancient individuals were used considering different sets of variants.

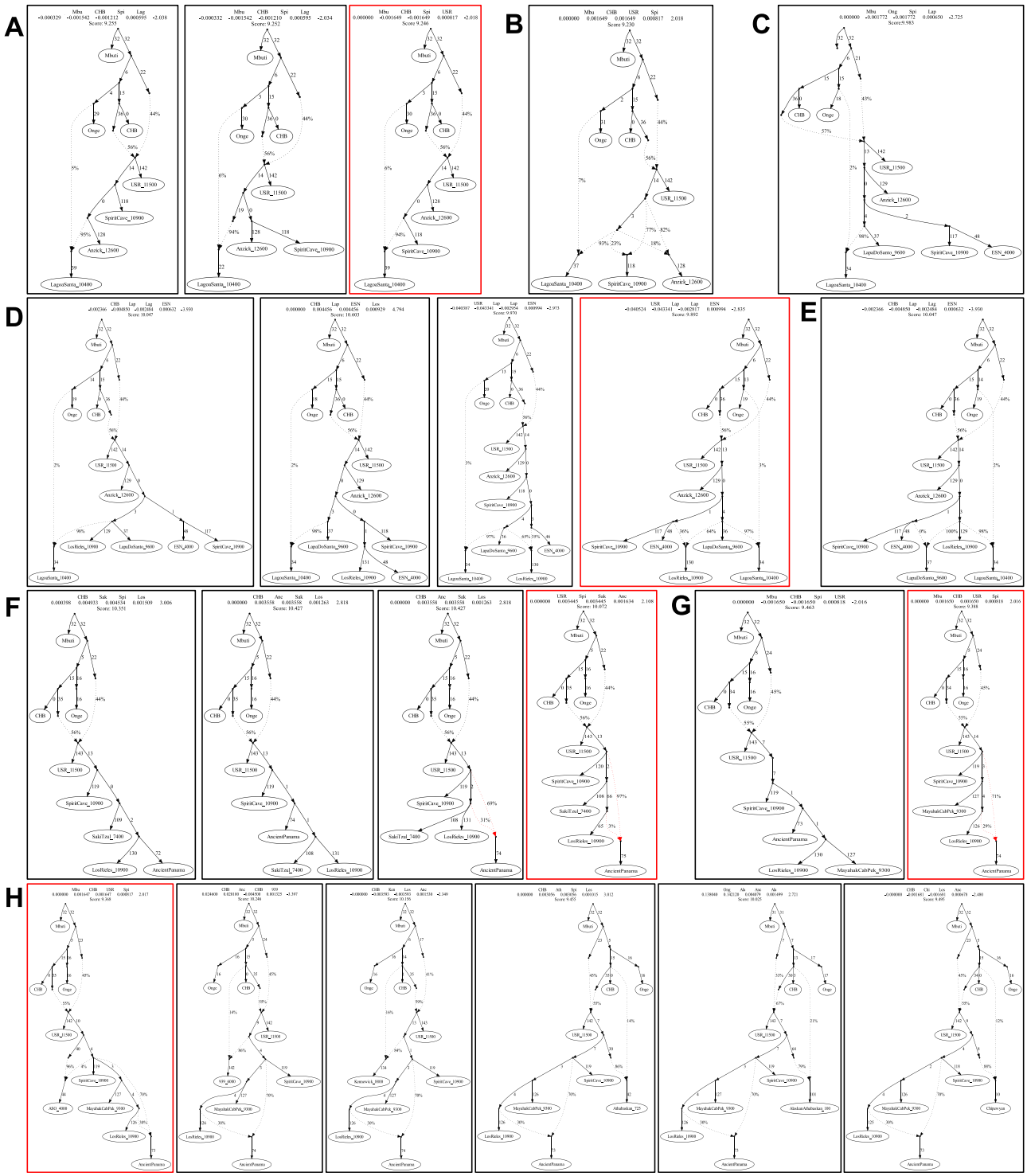

Figure S6. Admixture graphs modeling ancient SNA and NNA genomes and ancient Isthmians, related to Figure 7

(**A**) Basal tree with three of the most ancient SNA genomes available. The best fitting topology, highlighted in red, was initially tested by (**B**) considering an early admixture between the northern American SNA genomes, then extended by adding in turn: (**C**) Lapa do Santos and ESN; (**D**) Los Rieles, tested as either unadmixed or admixed, and then checking Lapa do Santos as admixed (**E**); ancient Isthmians together with other ancient Central American genomes, i.e., (**F**) Saki Tzul and (**G**) Mayahak Cab Pek; (**H**) NNA genomes, from the left to right, ASO, 939, Kennewick, Athabaskan_725, Athabaskan_100 and Chipewyan. The best fitting topologies are highlighted in red. See the legend of Figure 7 for further details.

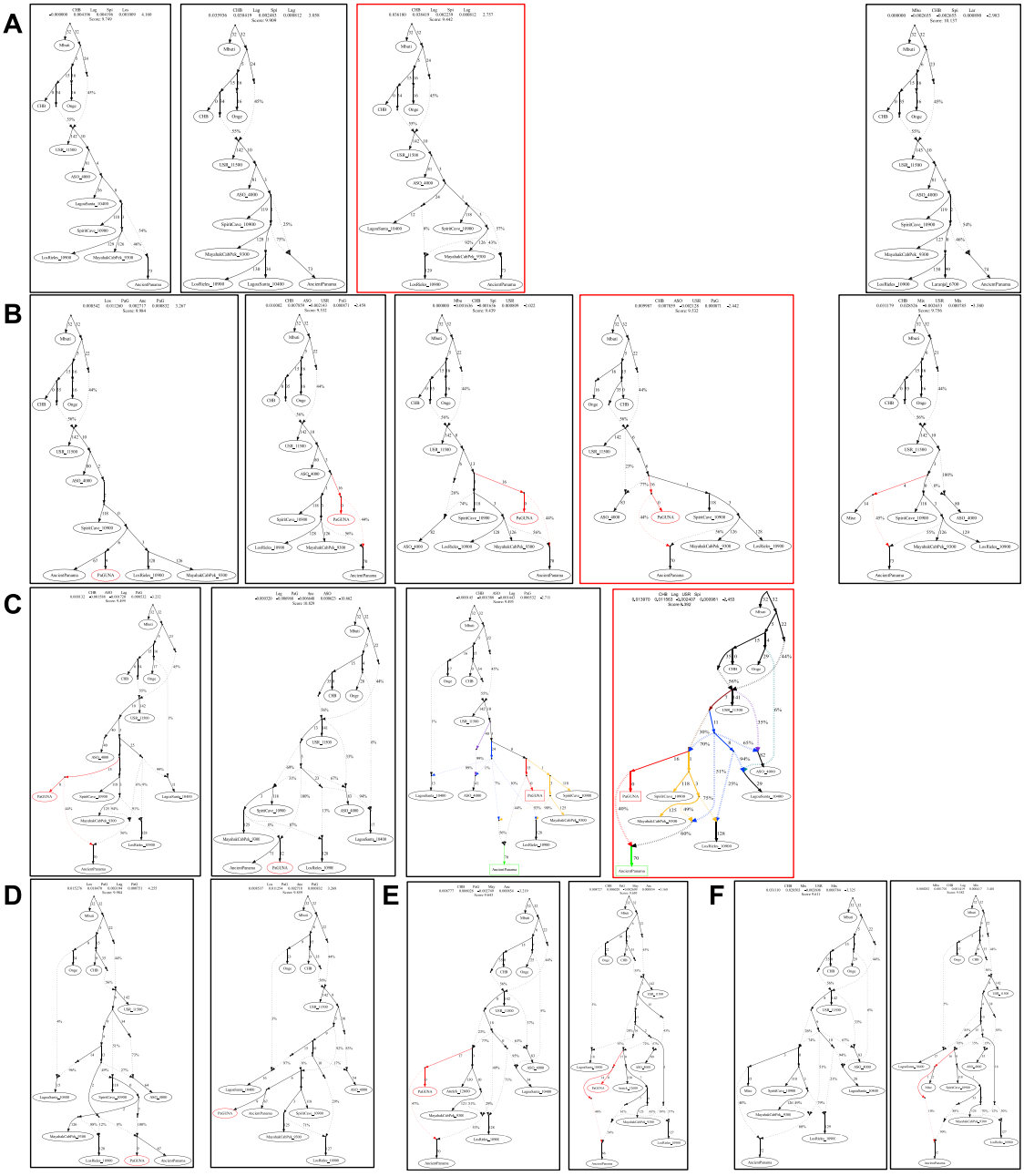

Figure S7. Admixture graph modeling Panama's genetic history linked to ancient SNA and NNA genomes, related to Figure 7

Possible extensions of the best trees in Figure S6 by linking Ancient Isthmians to (**A**) Lagoa Santa and then testing Laranjal instead of Lagoa Santa (rightmost graph). Finally, we modeled Guna as representative of UPopI **(B-C)**. The best tree topology is similar to the one in Figure 7, but with multiple splits from the SNA1 node. This tree as well as the final one (Figure 7) were checked multiple times: (**D**) considering Mixe (UPopA) instead of Guna (UPopI), also in the rightmost tree of the panel B; (**E**) replacing Spirit Cave with Anzick-1; (**F**) without UPopI or without admixture between UPopI and other SNA ancestries. The best fitting topologies are highlighted in red. See the legend of Figure 7 for further details.